Université Dr Moulay Tahar de Saida
Eberhard Karls Universität Tübingen

Faculty of Sciences

Institute of Physical and Theoretical Chemistry

Master thesis

Understanding the intermolecular interaction of the acceptor-donor complex Tetracyanobenzene(TCNB)-Benzene

Presented by
DELLAS Fatima Zohra

Under the direction of
Prof. Dr. rer. nat. Reinhold F. Fink

Tübingen, Germany 2023

Contents

1 Acknowledgement

In the name of Allah, the Most Gracious, the Most Merciful, I begin this acknowledgment section with gratitude in my heart for the countless blessings that have guided my academic journey. I am humbled and thankful to have had the opportunity to pursue my Master's thesis in Germany, under the esteemed guidance of Prof. Dr. rer. nat. Reinhold F. Fink.

I offer my deepest appreciation to my beloved family—my dad, mom, and sisters—for their unwavering support, love, and faith in my aspirations. Their encouragement has been my constant motivation.

I am indebted to Prof. Dr. rer. nat. Reinhold F. Fink for his invaluable guidance and mentorship throughout this journey.

To my professors and mentors in Algeria, including Professor Prof. Dr. Rahmouni Ali, I extend my sincere gratitude for imparting valuable knowledge and nurturing my academic growth. Your teachings have been instrumental in shaping my path.

I am also grateful to my dear friends, both in Algeria and Germany, whose friendship and support have added joy and camaraderie to this academic journey. I particularly want to express my appreciation to Michael Thelen and Johannes Henrichsmeyer, who have been instrumental in helping me with my thesis.

I also extend my thanks to Amel and Djamil, my fellow students in Germany, for their camaraderie and shared experiences that have enriched my time here.

Alhamdulillah, this thesis represents a collective effort, and I am thankful to every individual who has contributed to my personal and academic development. Your guidance, encouragement, and presence have been a blessing, and I am profoundly appreciative for your role in my life.

Abstract

This study focuses on obtaining the most stable configurations of TCNB-Benzene complexes using SAPT0 calculations. Geometrical models were employed, and calculations were performed based on fixed separations between the monomer planes. The role of exchange repulsion in determining the minimum intermolecular interaction and aggregate stability was established. Subsequently, orbital contributions were investigated using the Wavels package to identify the key orbitals involved in stabilizing the minimum structure. The analysis of these orbitals provides valuable insights into their specific roles and their overall influence on the system's stability. This research enhances our understanding of intermolecular interactions and paves the way for the design of more stable molecular systems.

2 Introduction

Noncovalent interatomic and intermolecular interactions play a fundamental role in determining the physicochemical properties of molecules and materials across various scientific domains, including chemistry, biology, and materials science. These interactions significantly impact molecular structures, dynamics, and functions. A comprehensive understanding of non-covalent interactions is essential for unraveling the behavior and properties of molecular systems, enabling the development of advanced materials, and advancing numerous applications.

Organic mixed crystals composed of electron donor and acceptor molecules exhibit intriguing properties related to electron conduction and coloration. These substances often form well-defined crystalline structures. Among these systems, 1,2,4,5-tetracyanobenzene (TCNB) is commonly studied as an acceptor molecule. The prevailing explanation for the preferred aggregate structure in donor-acceptor systems assumes strong interaction between the highest occupied molecular orbital (HOMO) of the donor and the lowest unoccupied molecular orbital (LUMO) of the acceptor. However, recent studies have challenged this simplistic explanation.

Mayoh and Prout (1972) [1] demonstrated that the overlap between the HOMO and LUMO orbitals in many donor-acceptor crystals is negligible. Instead, they found that charge-transfer stabilization involving other orbitals plays a significant role in stabilizing the crystal structures, though not all structures are stabilized in this manner. Therefore, understanding the intermolecular interactions in these crystals is of utmost importance for elucidating their molecular structures. Theoretical approaches can aid in unraveling the nature of these interactions, and energy component analysis allows for the examination of contributions

from various intermolecular forces, including electrostatics, London dispersion, induction (polarization), and short-range exchange-repulsion. Symmetry-adapted perturbation theory (SAPT) provides a method for such analyses.[2]

In the context of explaining aggregate structures, electrostatic interactions, induction, dispersion, and exchange-repulsion energy from SAPT0 calculations are considered. Repulsive electrostatic interactions, as proposed by the Hunter-Sanders model [3], play a crucial role in preventing the formation of eclipsed (sandwich) structures between two equal π-systems at their van der Waals distance,[4] which is not the sole determinant in our specific case.

In this project the energy decomposition method is used to gain better insight into the structure of acceptor-donor complexes. Our goal is to analyze the specific energy contributions that give rise to the observed planar stacking arrangements in crystal structures. Of particular interest is the investigation of the exchange-repulsion component, which has not been explored in much detail. By investigating orbital contributions to the exchange-repulsion energy, we aim to gain insights into its influence on the formation and stability of planar stacking interactions.

3 Theoretical Background

3.1 Ab Initio methods

The programs used in Quantum Chemistry are based on different quantum-mechanical methods that solve the molecular Schrödinger equation associated with the molecular Hamiltonian. Methods that do not include empirical or semi-empirical parameters in their equations are derived directly from theoretical principles and they are generally called ab initio methods.

One of the most basic ab initio electronic structure approaches is called the Hartree-Fock (HF) method, in which the Coulombic electron-electron repulsion is taken into account in an averaged way (mean field approximation). This is a variational calculation, therefore the obtained approximate energies, expressed in terms of the system's wavefunction, are always equal to or greater than the exact energy, and tend to a limiting value called the Hartree-Fock limit. Many types of calculations begin with a HF calculation and are subsequently corrected for the missing electronic correlation. Møller-Plesset perturbation theory (MP) and Coupled Cluster (CC) are examples of such methods[5]

3.2 Symmetry-Adapted Perturbation Theory: Back-ground.

The traditional theoretical method for calculating the intermolecular interaction energy E_{int} between two systems is the so-called supermolecular approach. In this method, the energies of the monomers E_A and E_B are subtracted from the energy of the dimer, E_{AB}, to give the total interaction energy E_{int} as:

$$E_{int} = E_{AB} - (E_A + E_B) \tag{1}$$

Unfortunately, E_{int} is typically many orders of magnitude smaller than the energies of the individual systems, and errors introduced by the applied approximations may be as large as the quantity sought. Even if the various theory and basis set truncation errors are smaller than the desired accuracy, the supermolecular method yields only one number, i.e., the total interaction energy, with no additional information about the physical nature of the interaction (e.g., electrostatic versus dispersive).[6]

The Symmetry-Adapted Perturbation Theory (SAPT) was developed as an ab initio approach to investigate weak interactions directly, and it has been successfully applied to various systems. In addition to its potential for high accuracy, SAPT provides a physically interpretable picture of the intermolecular interaction potential energy surface, as it naturally decomposes the total interaction energy (E_{int}) into components arising from electrostatic, exchange, inductive, and dispersive interactions between the two systems. By employing a suitable choice of atomic orbital (AO) basis set, SAPT components can be calculated more efficiently compared to an equivalent level of ab initio theory using the supermolecular approach . However, SAPT and other ab initio electron correlation methods are computationally demanding, largely due to the calculation of intramolecular correlation corrections.[6]

3.3 Symmetry-Adapted Perturbation Theory: Outline of the Theory.

A detailed derivation and description of SAPT has already been presented [7]-[8],[9]and will not be repeated here.The basic Hamiltonian used for SAPT is divided into two parts. The first, $H_0 = H_A + H_B$, represents the Hamiltonians for two isolated systems A and B. The second part is the intermolecular interaction operator V between the two systems. Adding

the two gives the full system Hamiltonian $H = H_0 + V$. Recent developments in wavefunction-based SAPT theory have made it possible to use SAPT approaches to varying degrees of completeness depending on the scale of the system being researched and the desired level of precision.

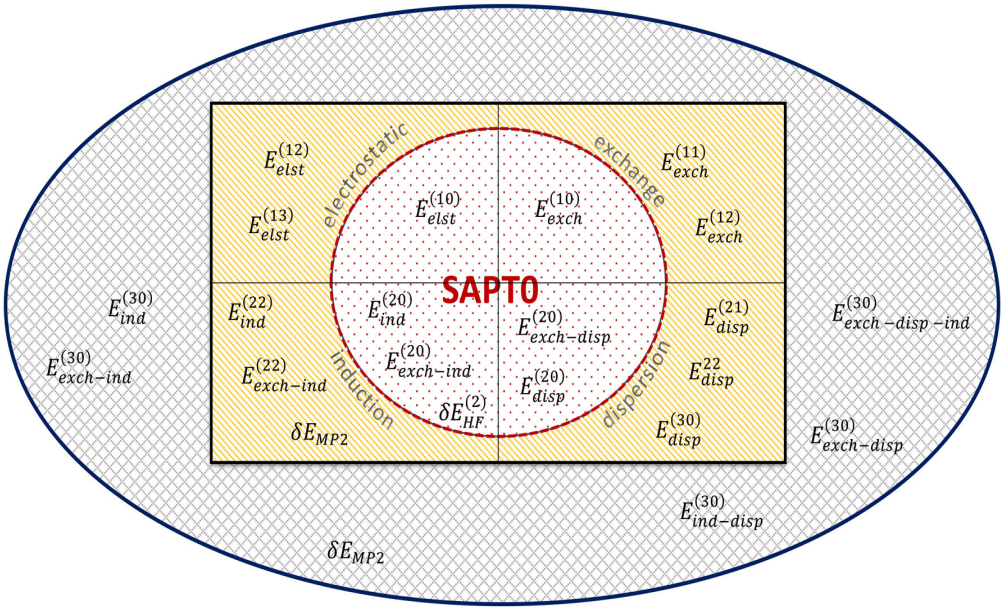

Figure 1: Terms contributing to the SAPT interaction energies: Inside the red circle are the terms considered using the SAPT0 method. The contributions inside the yellow area correspond to SAPT2+(3)δMP2, also known as gold- SAPT, and the highest level, SAPT2 + 3(CCD)δMP2, inside the oval line diamondSAPT. SAPT0 terms are only included inside the red circle (7 terms), gold- SAPT terms inside the rectangle(17 terms), and diamond–SAPT are inside the blue oval line (22 terms).[10]

Figure 1 present a pictorial description of the various contributions considered for the commonly used SAPT levels of theory.[10]

3.4 SAPT0

SAPT partitions the supramolecular Hamiltonian into a zeroth order part consisting of monomer Fock operators, plus Møller-Plesset fluctuation potentials (representing intramolec-

ular electron correlation), and finally intermolecular Coulomb operators.[11]-[12]Taking the latter perturbation to second order, with Hartree-Fock (HF) wave functions used to describe the isolated monomers, results in a method called "SAPT0".[11],[13] The corresponding partitioning of E_{int} is

$$E_{int}^{SAPT0} = E_{elst}^{(1)} + E_{exch}^{(1)} + E_{ind}^{(2)} + E_{exch-ind}^{(2)} + E_{disp}^{(2)} + E_{exch-disp}^{(2)} + \delta E_{HF} \tag{2}$$

Each term represents a physically meaningful contribution:[14]

- **Electrostatics:** $E_{elst}^{(1)}$ is the Coulomb interaction between the isolated-monomer charge densities.

- **Exchange:** $E_{exch}^{(1)}$ is the penalty for enforcing antisymmetry between monomer wave functions, which is known as Pauli repulsion.

- **Induction:** Polarization of the monomer charge densities is captured in

$$E_{ind} = E_{ind}^{(2)} + E_{exch-ind}^{(2)} + \delta E_{HF} \tag{3}$$

  Where δE_{HF} represents a correction for higher-order induction, as described below. (For separation of induction into polarization and charge-transfer contributions, see refs [15] and [16].)

- **Dispersion:** As originally described by London, [17] dispersion arises at second order in perturbation theory

$$E_{disp} = E_{disp}^{(2)} + E_{exch-disp}^{(2)} \tag{4}$$

due to correlation-induced fluctuations in the mean-field electron densities of the monomers.

The terms $E^{(1)}_{elst}$, $E^{(2)}_{exch-ind}$ and $E^{(2)}_{exch-disp}$ arise from antisymmetrization of the monomer wave functions and serve to remove Pauli-forbidden contributions to $E^{(1)}_{elst}$, $E^{(2)}_{ind}$ and $E^{(2)}_{disp}$, respectively.[18]

4 Computational Methodology

To investigate the structure of donor-acceptor complexes involving tetracyanobenzene (TCNB) as the donor molecule, Symmetry-Adapted Perturbation Theory (SAPT0) was employed. The aim was to calculate and compare the contribution of interaction energies in the TCNB-Benzene dimer.

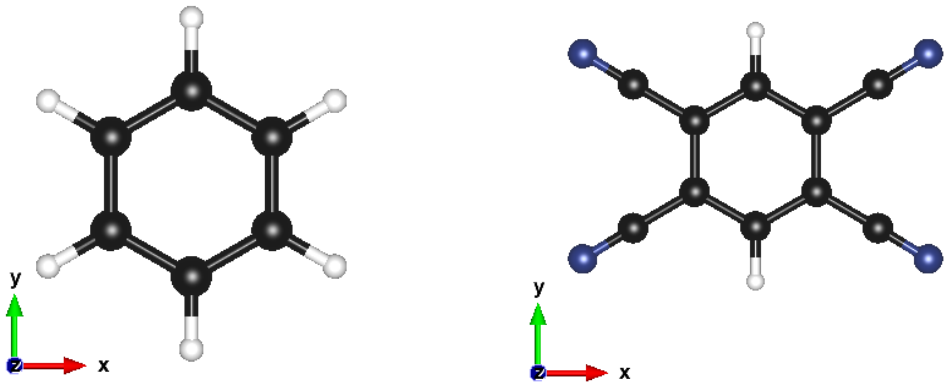

(a) Benzene (b) TCNB

Figure 2: Top view of optimized structure of: a) Benzene, b)TCNB at the MP2/aug-cc-pVTZ level of theory.

The initial step involved optimizing the equilibrium geometries of the two monomers, TCNB and benzene, using the resolution of identity in the second-order Møller-Plesset method (MP2) along with the aug-cc-pVTZ basis set as it is shown in figure 2. The calculations were conducted using the TmoleX/Turbomole software [19] .

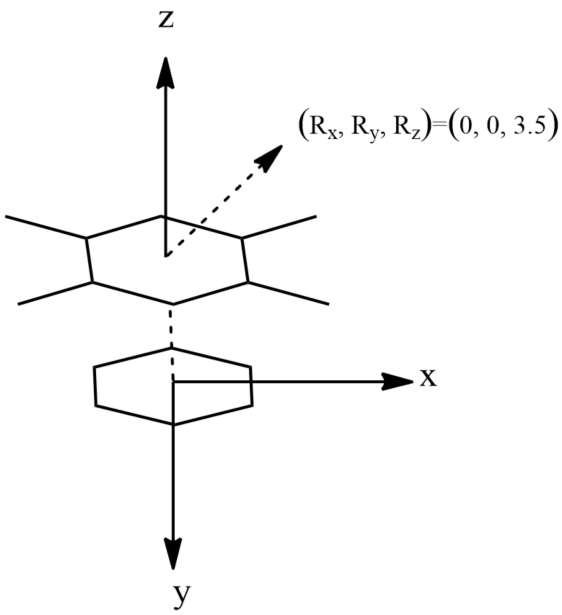

Figure 3: Representative conformations of the TCNB-benzene dimer

To obtain the most stable configurations of the TCNB-Benzene complexes, we employed SAPT0 calculations, for geometrical models shown in figure 3 , where the center of the benzene is taken as an origin of the coordinate system and R_x, R_y and R_z are the coordinates of the center of the benzene ring of TCNB, the separtion between the two monomers is fixed at $R_z = 3.5$ Å. Initially, we determined this distance to have the minimal for x=y=0. Subsequently, calculations were performed for the X, Y, and XY planes. The jun-cc-pVDZ basis set was utilized for these calculations which were carried out using the Psi4 software package [20] .

Having established the significant role of exchange repulsion in determining the minimum intermolecular interaction and stability of the aggregate, we employed the Wavels package to perform calculations and investigate the orbital contributions. Our objective was to discern the specific orbitals that play a crucial role in stabilizing the structure and further analyze

their contributions.

Through the utilization of the Wavels package, we obtained orbital-orbital contributions to the interaction energy and conducted a detailed study to identify the orbitals that contribute significantly to the stabilization of the structure. This investigation allowed us to gain insights into the specific orbitals' roles and their influence on the overall stability of the system.

5 Results and Discussion

5.1 Geometry Optimization

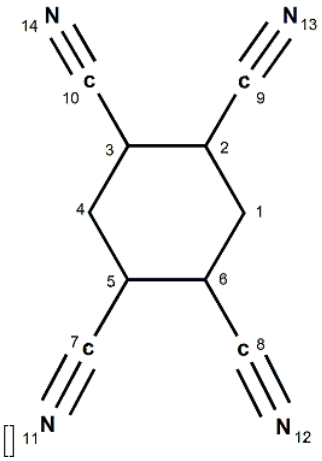

Figure 4: Projection on the molecular plane showing atom numbering

Bond length	^{a}exp	$^{b}MP2$	error
$C_1 - C_2$	1.381	1.401	$\pm$ 0.02
$C_1 - C_6$	1.381	1.401	$\pm$ 0.02
$C_2 - C_3$	1.425	1.416	$\pm$ 0.009
$C_2 - C_9$	1.450	1.4336	$\pm$ 0.0164
$C_9 - N_{13}$	1.127	1.180	$\pm$0.053
Angle			
$C_1 - C_2 - C_9$	1.381°	1.401°	$\pm$ 0.1
$C_3 - C_2 - C_9$	1.381°	1.401°	$\pm$ 1
$C_1 - C_2 - C_3$	1.425°	1.416°	$\pm$ 1
$C_2 - C_9 - N_{13}$	1.450°	1.4336°	$\pm$ 0.5
$C_2 - C_1 - C_6$	1.127°	1.180°	$\pm$ 1.9

Table 1: Experimental[21] and Calculated structure of TCNB (*a:The crystal structure of TCNB with Naphthalene. *b: aug-cc-pVTZ basis set).

In order to evaluate the accuracy of our computed geometry of the TCNB, we have compared it with the experimental one [21], as it is shown in the table 5.1. the error shows that they are in good qualitative agreement with the results obtained with the MP2 method if we take into account that the experimental and theoretical structure of TCNB was taken from a different complex, which is TCNB-benzene and TCNB-naphthalene, respectively.

5.2 Interaction energy contribution from Symmetry Adapted Perturbation Theory (SAPT0)

The SAPT0 interaction energy is a sum of four contributions, including induction, exchange, electrostatic and dispersion, therefore it is the most efficient method for quantifying the intermolecular interaction in our case. For the acquisition of the preferred aggregates, we have done the calculation by shifting along different axis and then analyze the interaction energy contributions that we get from SAPT0.

5.2.1 SAPT0 calculation along Z axis

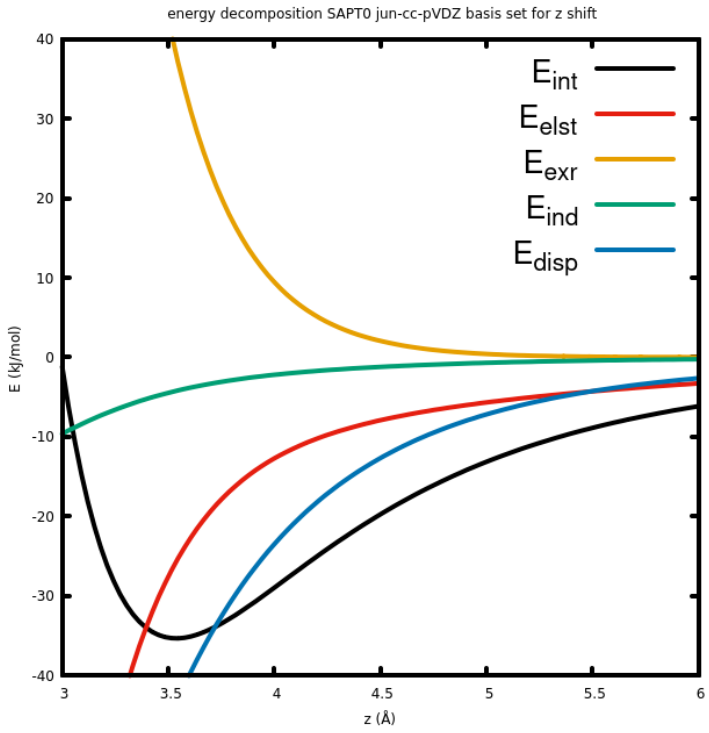

Figure 5: SAPT0/jun-cc-pVDZ interaction energy and its constituent energy components (electrostatics, exchange-repulsion, induction, and dispersion) for an increase distance along z-axis.

The SAPT0 results for the Z-shift, ranging from 3 to 6 Å with a step size of 0.1 Å, are depicted in Figure 5. As the separation between the two monomers increases, the total energy initially decreases to a minimum at 3.5 Å and then rises with further increase of z. Among the four components of intermolecular interactions, the negative one represent attractive interactions, while the positive E_{exr} curve indicates repulsive interactions. The negative sign of the total energy (represented by the black curve) indicates the dominance of attractive forces over repulsive forces. Note that this SAPT0 minimum occurs between 3 and 4.5 Å in this range the electrostatic and dispersion interactions are similar in magnitude, with dispersion dominating the stabilising energy components at short range and electrostatics dominating at extremely long range. The exchange repulsion is strongly repulsive when the two monomers are close to each other and then decreases as the distance between the dimer increases.

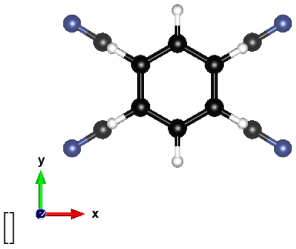

[]

Figure 6: Structure of the dimer TCNB-Benzene

contribution	Energy ($kJ.mol^{-1}$)
E_{exr}	42.53
E_{elst}	-27.56
E_{ind}	-4.47
E_{disp}	-45.74
E_{tot}	-35.23

Table 2: Contributions to the interaction energy ($kJ.mol^{-1}$) using SAPT0. in the distance of the minimum interaction energy in z-shift of 3.5 Åbetween the TCNB-Benzene. Eelec , Eexch , Eind , and Edisp stand for the electrostatic, exchange, induction, and dispersion contributions, respectively. Etot stands for the total interaction energy

The contributions of the intermolecular interaction at the equilibrium distance Z=3.5Å (corresponding to the minimum total energy E_{int}=-35.23 $kJ.mol^{-1}$), are summarized in Table 5.2.1 , the attractive component values include E_{elst} (-27.56 $kJ.mol^{-1}$: 35%),E_{ind}(-4.47 $kJ.mol^{-1}$: 6%) and E_{disp} (-45.74 $kJ.mol^{-1}$: 59%). These values indicate that the dispersion energy plays a significant role in stabilization compared to the electrostatic and induction energies.

5.2.2 SAPT0 calculation along X axis

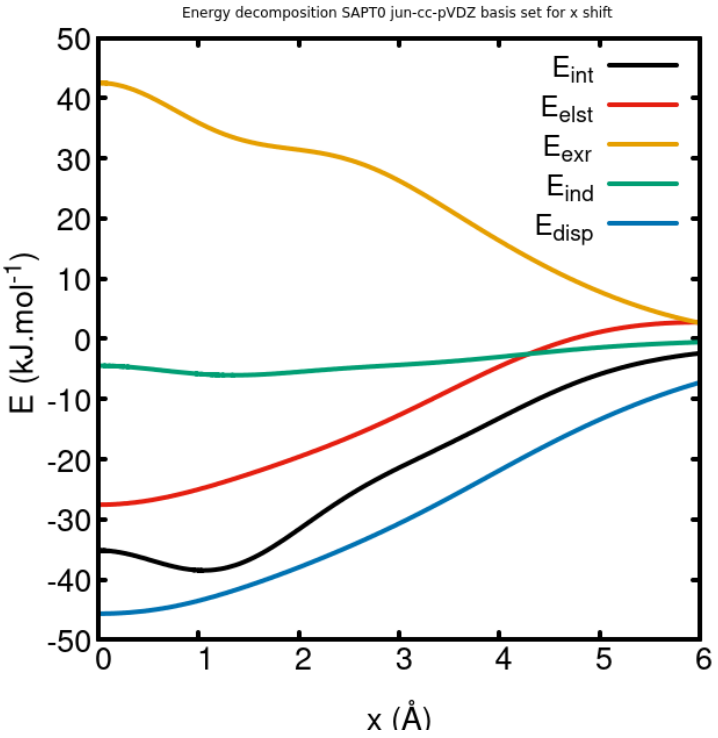

Figure 7: SAPT0/jug-cc-pVDZ interaction energy and its constituent energy components (electrostatics, exchange-repulsion, induction, and dispersion) for shift along x-axis with z=3.5 Å.

The shift in the x-axis, is depicted in Figure 7 showing a minimum in the total intermolecular interaction occurring at approximately $x \approx 1.0$ Å, spanning a range of 0 to 2.5 Å, which is

approximately 5 $kJ.mol^{-1}$ below the x=0 Å value. Notably, the dominant factor contributing to the stabilization of the complex is the dispersion energy, exhibiting a similar trend and magnitude as the electrostatic interactions. This observation holds true across the entire range of the shift. Additionally, the induction contribution displays a small minimum at the same distance as the overall SAPT0 total interaction minimum, albeit with an average of approximately 1.5 $kJ.mol^{-1}$ (absolute value). Interestingly, within this range, the exchange repulsion demonstrates a distinct deviation. From these findings, it can be inferred that the minimum in intermolecular interaction primarily arises from the contribution of exchange repulsion.

contribution	Energy ($kJ.mol^{-1}$)
E_{exr}	35.89
E_{elst}	-25
E_{ind}	-5.83
E_{disp}	-43.51
total interaction	-38.45

Table 3: Contributions to the interaction energy ($kJ.mol^{-1}$) using SAPT0. in the distance of the minimum interaction energy in x-shift of 1 Åbetween the TCNB-Benzene. Eelec, Eexch, Eind, and Edisp stand for the electrostatic, exchange, induction, and dispersion contributions, respectively. Etot stands for the total interaction energy

Table 3 provides a detailed breakdown of the various contributions to the total energy at the minimum (-38.45 $kJ.mol^{-1}$) occurring at x = 1 Å. The dispersion interaction accounts for 58.53% of the attractive energy, which is approximately half of the total. The electrostatic contribution follows with 33.63%, and the induction component contributes 7.84% to the total attractive energy.

5.2.3 SAPT0 calculation along Y axis

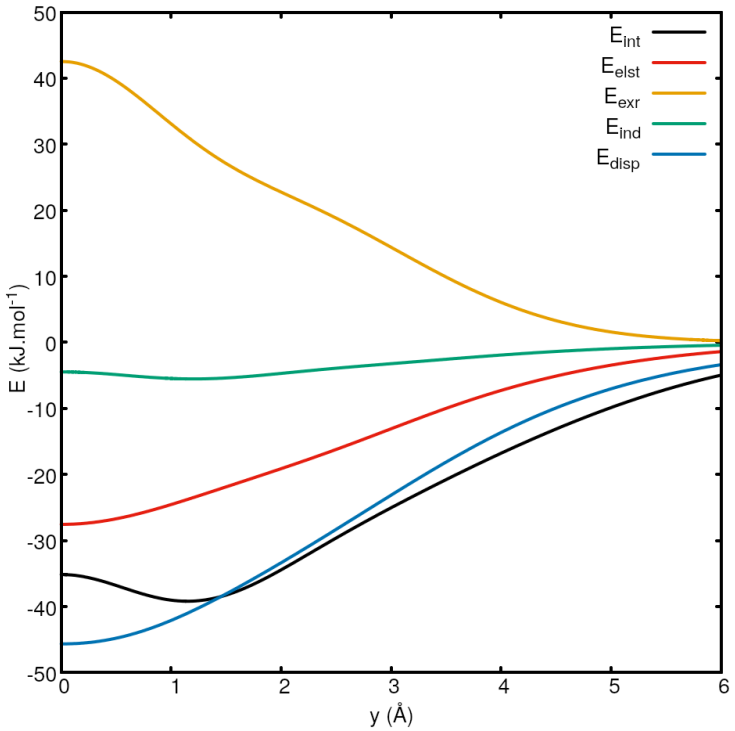

Figure 8: SAPT0/jun-cc-pVDZ interaction energy and its constituent energy components (electrostatics, exchange-repulsion, induction, and dispersion) for shift along y-axis with z=3.5 Å.

Upon analyzing a shift along the y-axis, Figure 8 illustrates a minimum in the total intermolecular interaction at approximately $y \approx 1.1$ Å, spanning a range of 0 to 3 Å. The average energy, with absolute value, amounts to approximately 4 $kJ.mol^{-1}$. Notably, the principal factor responsible for stabilizing the complex (all of the attractive contributions) is the dispersion energy , displaying a similar pattern and magnitude as the electrostatic interactions. In the shorter ranges, both interactions contribute to attraction, but beyond the interaction minimum, the dispersion energy decreases more rapidly. Furthermore, the induction contribution exhibits a minor minimum at the same distance as the overall SAPT0

total interaction minimum, averaging approximately 1.0 $kJ.mol^{-1}$ (absolute value). Remarkably, within this range, the exchange repulsion demonstrates a slight but notable deviation. Based on these findings, it can be inferred that the minimum in intermolecular interaction predominantly arises from the influence of exchange repulsion.

contribution	Energy ($kJ.mol^{-1}$)
E_{exr}	31.75
E_{elst}	-24.03
E_{ind}	-5.52
E_{disp}	-41.37
total interaction	-39.17

Table 4: Contributions to the interaction energy ($kJ.mol^{-1}$) using SAPT0. in the distance of the minimum interaction energy in y-shift of 1.1 Å. E_{elec}, E_{exch}, E_{ind}, and E_{disp} stand for the electrostatic, exchange, induction, and dispersion contributions, respectively. Etot stands for the total interaction energy

Table 4 details the various contributions to the total energy of the minimum (-39.17 $kJ.mol^{-1}$) that occurs at y = 1.1 Å. The analysis reveals that the dispersion interaction dominates, contributing 58.33% of the total attractive energy. Following closely is the electrostatic component, accounting for 33.88% of the overall attraction. The inductive contribution is relatively smaller, representing 7.78% of the total attractive energy.

5.2.4 SAPT0 calculation along XY plane

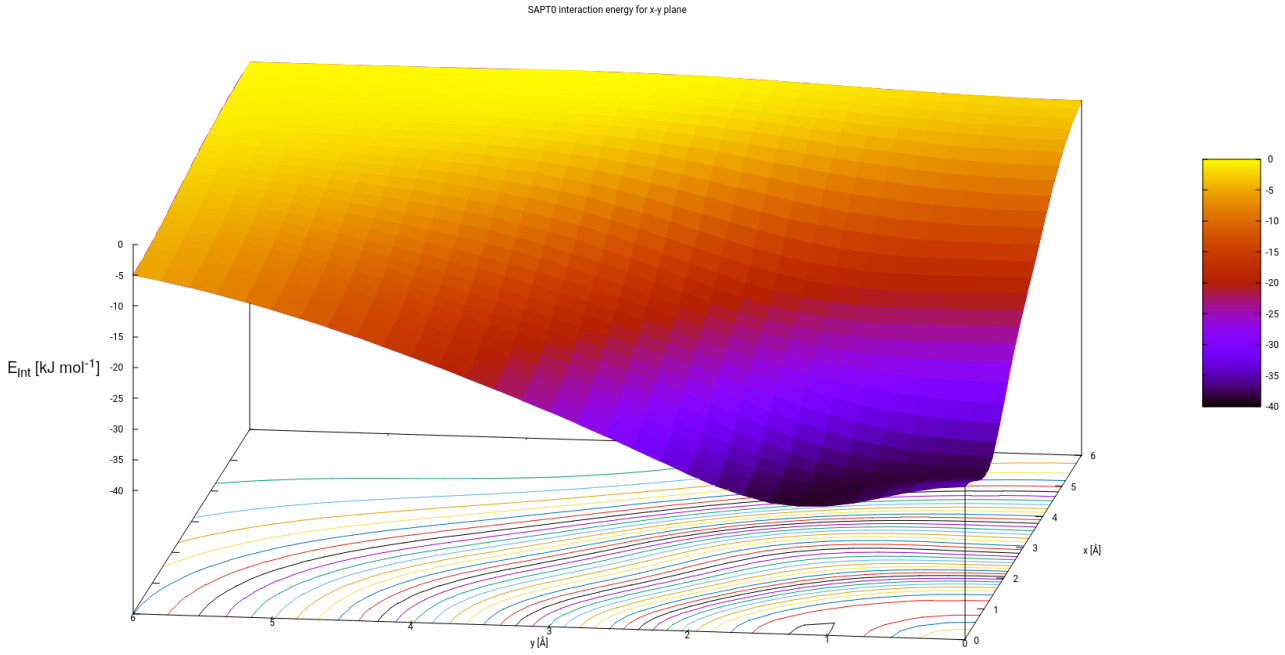

Figure 9: 2D and contour plot of the intermolecular interaction energy surface (E_{int}in $kJ.mol^{-1}$) as a function of the distances x and y (in Å).

In our study, we opted to investigate the intermolecular interaction surface along the xy plane. By analyzing the data presented in Figure 9 , we observe that the minimum value of the intermolecular interaction lies within the range of x=1.0 and y=1.1, with a global minimum found at x=0 Å, y=1.1 Å .

This analysis allows us to identify the specific region within the xy plane where the intermolecular forces are most favorable, indicating the preferred stable structure of the dimer. The presence of a global minimum in the y-direction suggests that the intermolecular interactions are particularly strong along this axis, leading to a more stable configuration. The range of x=1 Å and y=1.1 Å represents the region of optimal interaction, where the

energy of the system is minimized.

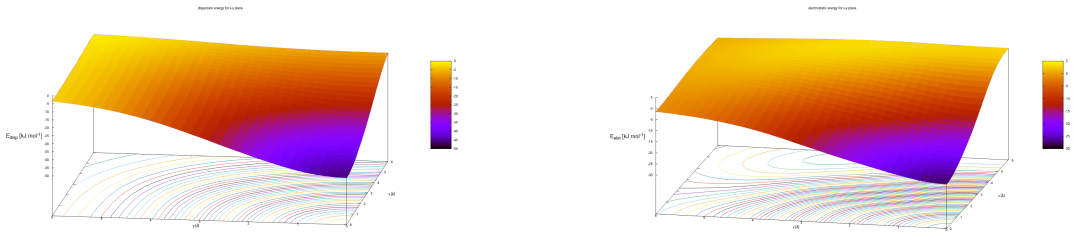

(a) Dispersion

(b) Electrostatic

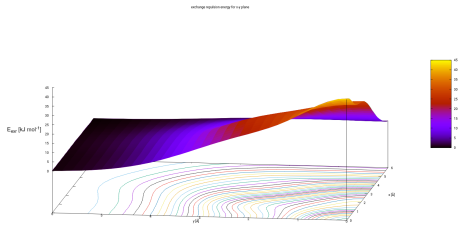

(c) Exchange-repulsion

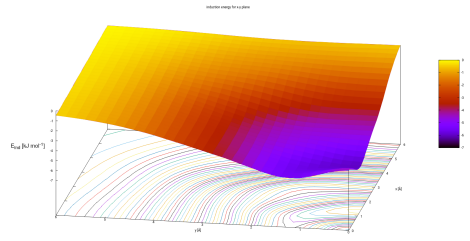

(d) Induction

Figure 10: 2D and contour plot of the different contributions of the intermolecular interaction energy surface (in $kJ.mol^{-1}$) as a function of the distances x and y (in Å).

Upon examining the surface plot (Figure 10) of the contribution energies along the xy plane, notable patterns emerge. The dispersion and electrostatic interactions display a global minimum at the coordinates (0,0), indicating their lowest energy values at the origin of the xy plane. Conversely, the induction contribution exhibits a global minimum along the x-axis, indicating its minimum energy value away from the origin.

Additionally, the exchange repulsion displays a maximum at the origin (0,0) and along the x-axis.

5.3 Orbital contribution Analysis

The main focus of this part is to shed new light on repulsive interactions by taking a closer look at the exchange-repulsion contribution specifically the orbitals contributions. The result of these calculations are shown in graphs with the variation of the total exchange repulsive energy (known as Pauli repulsion energy) and its different occupied orbitals contributions (from $\sigma - \sigma$, $\sigma - \pi$ to $\pi - \pi$) in terms of the intermolecular distance.

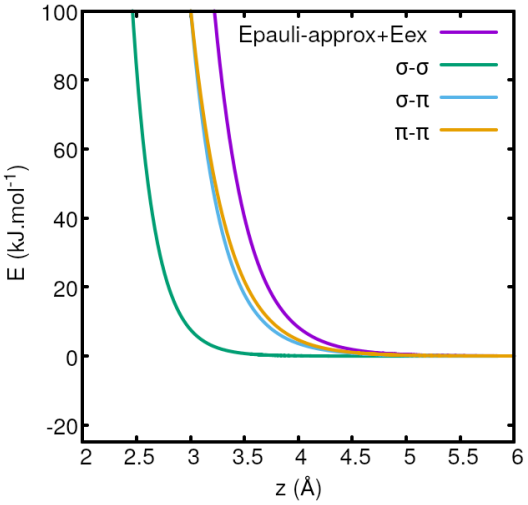

Figure 11: Different orbitals contributions and exchange repulsion versus the intermolecular distance of the shifting along z-axis

The results of the shift along the z-axis in Figure 11 are somewhat unsurprising, since the distance is the controlling factor in the staking structure, so the overlap between the electron orbitals is so strong specially the orbitals surrounding each molecule , thus causing that the $\sigma - \sigma$ component in the short displacement stacked dimer (z=2.5 Å) is dominant, while around 3.5 Å the $\sigma - \pi$ and $\pi - \pi$ contributions are the dominants

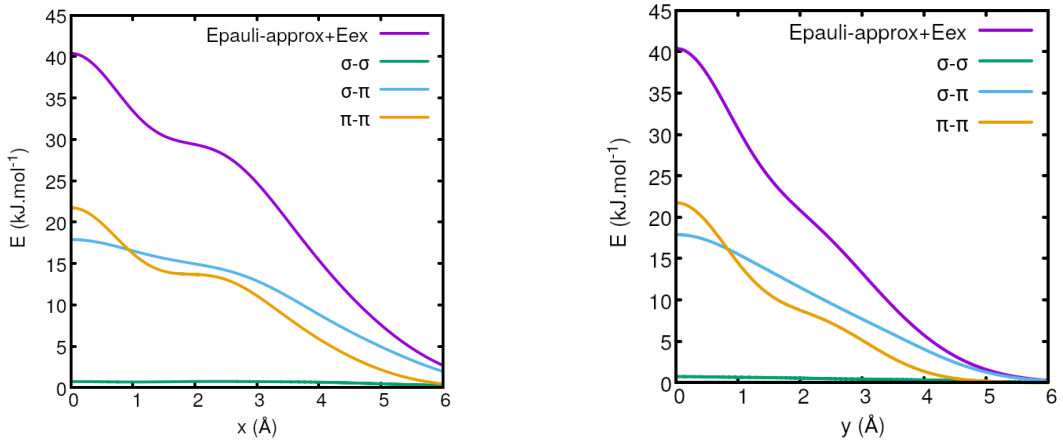

(a) (b)

Figure 12: Different orbitals contributions and exchange repulsion versus the intermolecular distance of the: a) shifting along x-axis b) shifting along y-axis

Based on the analysis of the graph depicting the interactions between x and y, several noteworthy observations can be made. Firstly, $\sigma - \sigma$ interactions, represented by the green curve, appear to be negligibly small compared to the other two interactions. The $\sigma - \pi$ interaction, denoted by the blue curve, exhibits considerable repulsion at short distances, gradually diminishing as the distance between the monomers increases. Notably, the rate of decrease along the x-axis is relatively gradual and slower compared to the y-axis shift.

Turning to the curve representing the $\pi - \pi$ interactions, it is strikingly similar in shape to the overall exchange repulsion interaction curve. It appears that the sholders of the exchange repulsion energies are essentially due to similar structures in $\pi - \pi$ contributions. This observation highlights the relation between the $\pi - \pi$ contribution and the exchange repulsion.

Based on these results, important conclusions can be drawn about the main factors determining the exchange-repulsion interactions. Obviously, these interactions are mainly controlled

by $\pi - \pi$ interactions. This conclusion is supported by the observed strong correlation between the shape of the $\pi - \pi$ interaction curve and the bulk exchange repulsion energy curve.

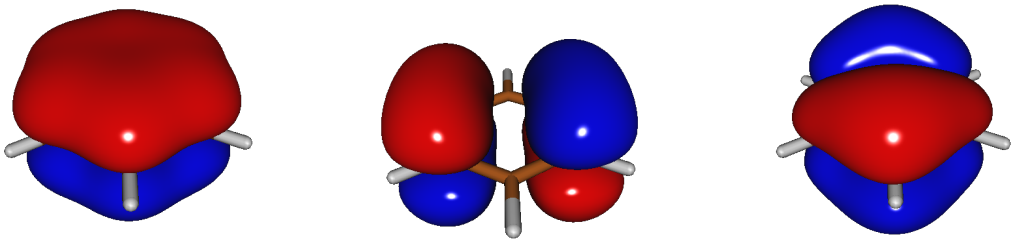

(a) a_{2u} (b) e_{1g_x} (c) e_{1g_y}

Figure 13: The occupied π-orbitals in benzene molecule

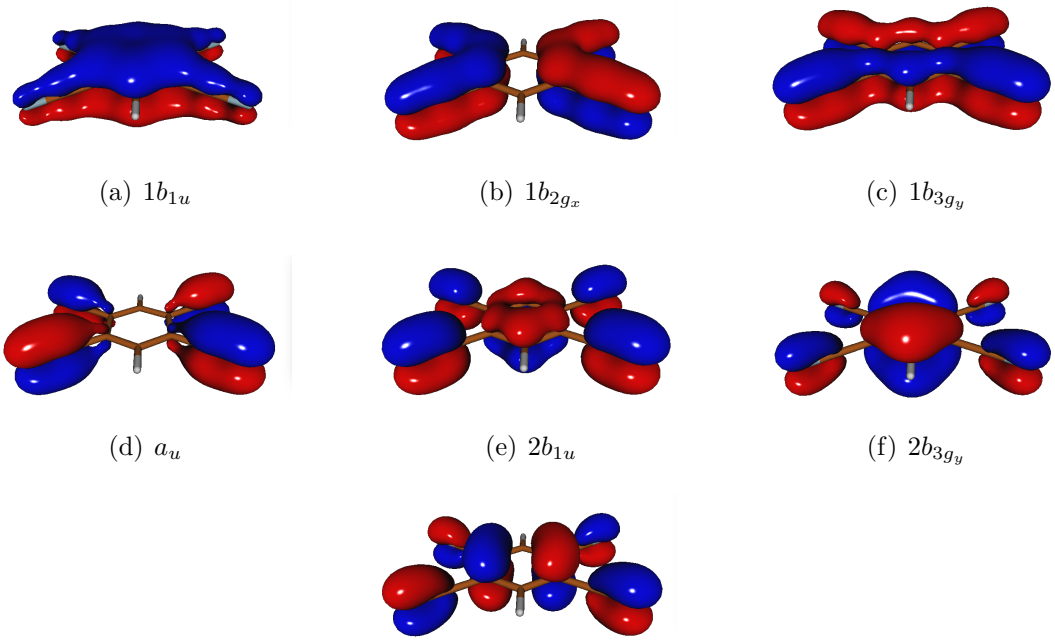

(a) $1b_{1u}$ (b) $1b_{2g_x}$ (c) $1b_{3g_y}$

(d) a_u (e) $2b_{1u}$ (f) $2b_{3g_y}$

(g) $2b_{2g_x}$

Figure 14: The occupied π-orbitals in TCNB molecule

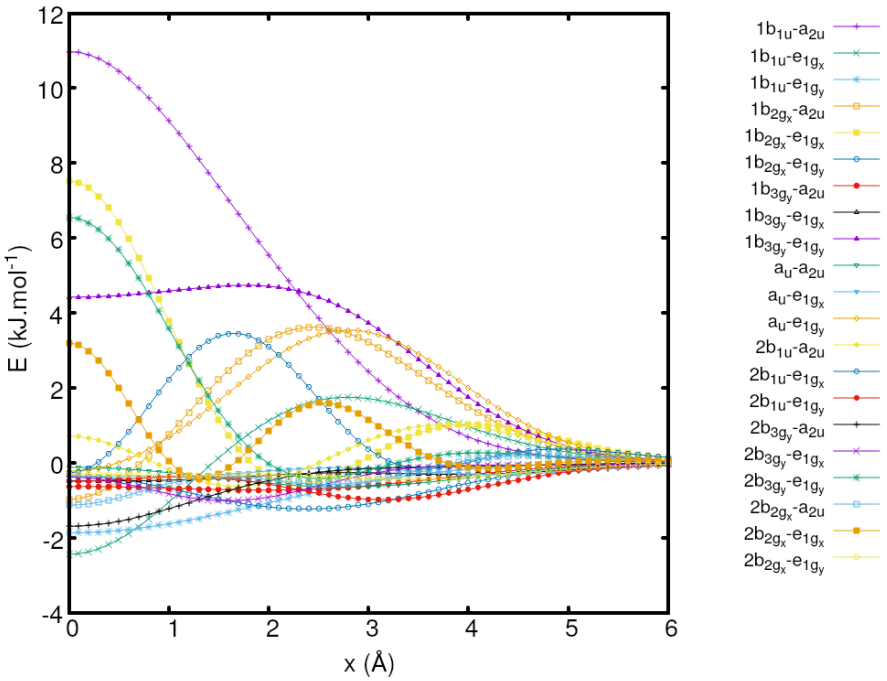

Figure 15: Analysis of the Contributions of Occupied π Orbitals in the TCNB-Benzene Dimer with x-axis shift

Figure 15 provides an analysis of the $\pi - \pi$ interactions between one π orbital from either of the systems (TCNB or benzene) with one π orbital from the other system with shifting along x-axis. By examining the graph, different types of $\pi - \pi$ interactions can be discerned. at x=0 (representing the stacking mode), highly repulsive interactions are observed, such as $1b_{2g_x} - e_{1g_x}$, and $2b_{3g_y} - e_{1g_x}$. These repulsive interactions arise from the substantial orbital overlap, whereby an increase in dimer distance resulted in a noticeable reduction in orbital overlap. Conversely, attractive interactions, such as $1b_{1u} - e_{1g_x}$, are also present, indicating zero overlap.

Furthermore, the graph reveals contributions that are nearly zero. These near-zero contributions do not significantly impact the behavior of the system as they neither exhibit strong repulsion nor attraction as $1b_{1u} - a_{2u}$ contribution.

The remarkable curves are those that characterized by their initial display of either repulsive or attractive behavior, which subsequently undergoes a behavioral shift as the distance between the interacting entities increases. A comprehensive understanding of these can be important for elucidating the fundamental properties and characteristics of intermolecular interactions, especially the contribution of exchange repulsion.

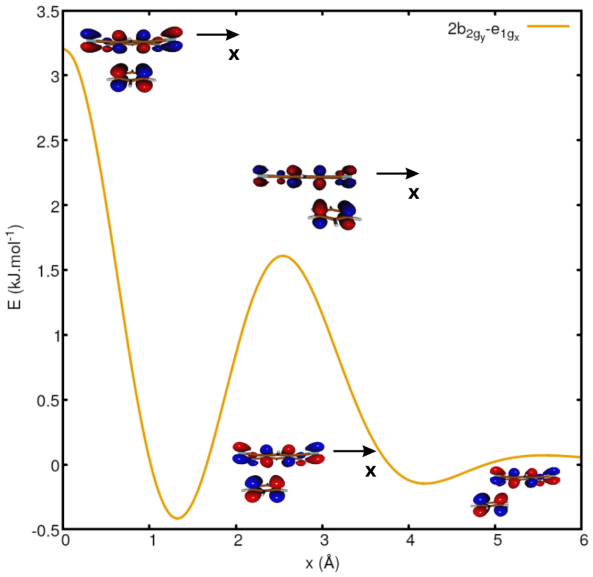

Figure 16: $2b_{2g_x} - e_{1g_x}$ contribution

Figure 16 provides a detailed analysis of the contributions of the occupied π orbitals, the $2b_{2g_x}$ orbital of TCNB and the e_{1g_x} orbital of benzene. Examining the orbital symmetries reveals that these orbitals share the same nodal structure (nodal plane perpendicular to the x-axis). In a face-to-face arrangement, the lobes of these orbitals overlap, resulting in a repulsive interaction. As the distance between the monomers increases, this overlap gradually decreases until it reaches a point of zero overlap ($x \approx 1.3$ Å). At this point, the interaction becomes slightly attractive. However, as the distance further increases $x \approx 2.5$

Å, the overlap turns positive again. Eventually, for larger values of x, the overlap becomes negative once more, reaching zero.

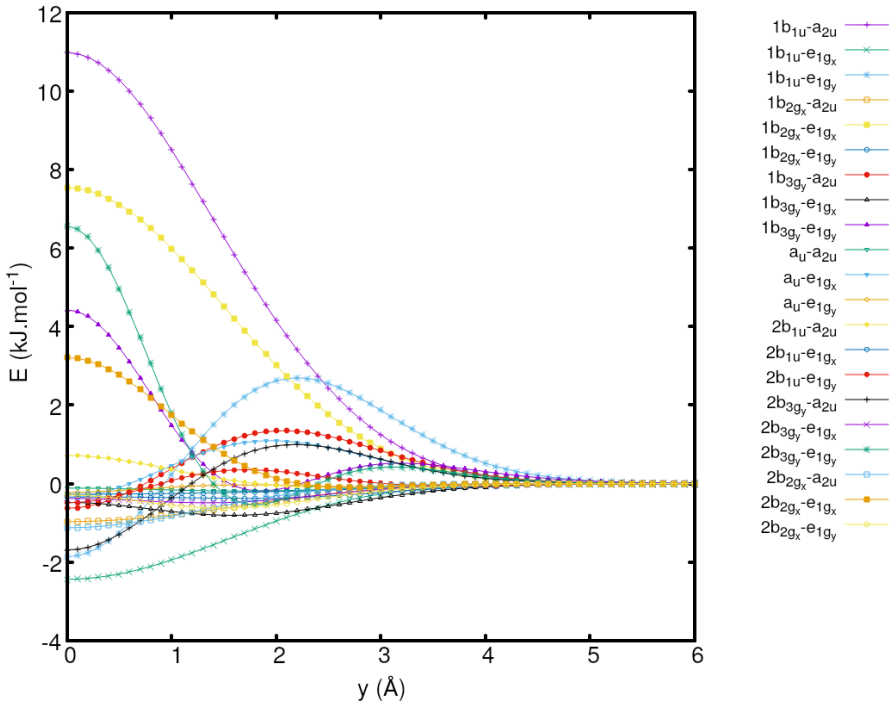

Figure 17: Analysis of the Contributions of Occupied π Orbitals in the TCNB-Benzene Dimer with y-axis shift

From figure 17 it is clear that as the shifting along x-axis the y-axis graph, various types of $\pi - \pi$ interactions can be discerned.In the stacking mode (x=0), the system exhibits highly repulsive interactions, specifically $1b_{2g_y} - e_{1g_x}$ and $2b_{3g_x} - e_{1g_x}$. These repulsive interactions arise due to the significant overlap between the corresponding orbitals. As the dimer distance increases along the y-axis, the magnitude of orbital overlap decreases noticeably, resulting in a reduction of the repulsive interactions. Conversely, attractive interactions, such as $1b_{1u} - e_{1g_x}$, are also evident, indicating zero overlap between the corresponding π orbitals.

The graph further exhibits contributions that are nearly zero. While these near-zero contributions have minimal impact on the system's behavior, as they neither display strong repulsion nor attraction. Particularly remarkable are the curves characterized by an initial display of either repulsive or attractive behavior, followed by a shift in behavior as the distance between the interacting entities increases. Gaining a comprehensive understanding of these distinctive curves is crucial for elucidating the fundamental properties and characteristics of intermolecular interactions, with a specific focus on the contribution of exchange repulsion.

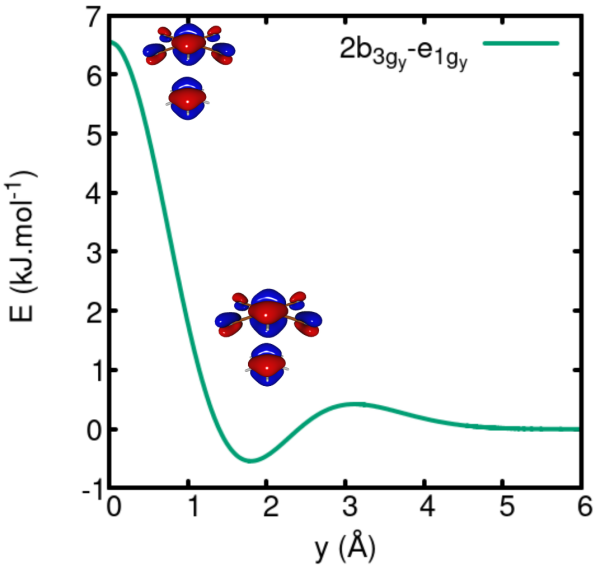

Figure 18: $2b_{3g_y} - e_{1g_y}$ contribution

Figure 18 presents a comprehensive analysis of the contributions from the occupied π orbitals, specifically the $2b_{3g_y}$ orbital of TCNB and the e_{1g_y} orbital of benzene. These orbitals share a common nodal structure, with a nodal plane perpendicular to the y-axis. In the face-to-face arrangement, the lobes of these orbitals overlap, resulting in a repulsive inter-

action. As the distance between the monomers increases, this overlap gradually diminishes, eventually reaching a point of zero overlap ($y \approx 1.8$ Å). At this critical point, the interaction undergoes a slight shift towards attraction. However, as the distance further increases ($y \approx 3.0$ Å), the overlap becomes positive again. Subsequently, for larger values of y, the overlap returns to zero.

6 Conclusion

In conclusion, our utilization of computational methodologies, such as SAPT0 and wavefunction analysis, has significantly enhanced our understanding of intermolecular interactions and their orbital contributions of the TCNB-benzene system. Through these approaches, we have gained valuable insights into the energy components that drive intermolecular forces in the context of the molecular orbitals of the interacting molecules.

In the specific case of the tetracyanobenzene-benzene system, our analysis has revealed the presence of a stable structure with a global minimum in the y shift. This finding highlights the significance of comprehending intermolecular interactions in determining the preferred arrangements and stability of molecular systems.

Furthermore, our investigation of energy decompositions and analysis of intermolecular interaction graphs have unveiled distinct patterns of repulsion, attraction, and changes in orbital overlap as a function of distance. Notably, our examination of individual orbital contributions, particularly $\pi - \pi$ orbitals, has provided essential insights into their specific roles in maintaining molecular stability.

Remarkably, our findings challenge the prevailing notion that as proposed by the Hunter-Sanders model electrostatic interactions, solely determine the observed planar stacking arrangements of molecular π systems. This suggests the necessity of a more comprehensive understanding of multiple factors, including the influence of exchange repulsion arising from orbital-orbital interactions, to accurately describe the energy landscape and behavior of the molecular systems under investigation

References

[1] B. Mayoh and C. K. Prout. "Molecular complexes. Part 13.—Influence of charge transfer interactions on the structures of π-π^* electron donor-acceptor molecular complexes". In: *J. Chem. Soc., Faraday Trans. 2* 68 (0 1972), pp. 1072–1082. DOI: 10.1039/F29726801072. URL: http://dx.doi.org/10.1039/F29726801072.

[2] C David Sherrill. "Energy component analysis of π interactions". In: *Accounts of chemical research* 46.4 (2013), pp. 1020–1028.

[3] Christopher A Hunter and Jeremy KM Sanders. "The nature of. pi.-. pi. interactions". In: *Journal of the American Chemical Society* 112.14 (1990), pp. 5525–5534.

[4] Johannes Henrichsmeyer et al. "Rationalizing Aggregate Structures with Orbital Contributions to the Exchange-Repulsion Energy". In: *ChemPhysChem* (2023), e202300097.

[5] Prof. Ursula Röthlisberger. *Introduction to ElectronicStructure Methods*. Tech. rep. EPFL, Lausanne, 2019.

[6] Hayes L. Williams and Cary F. Chabalowski*. "Using Kohn-Sham Orbitals in Symmetry-Adapted Perturbation Theory to Investigate Intermolecular Interactions". In: *J. Phys. Chem. A* (2001).

[7] Bogumil Jeziorski, Robert Moszynski, and Krzysztof Szalewicz. "Perturbation theory approach to intermolecular potential energy surfaces of van der Waals complexes". In: *Chemical Reviews* 94.7 (1994), pp. 1887–1930.

[8] Hayes L Williams et al. "Dispersion energy in the coupled pair approximation with noniterative inclusion of single and triple excitations". In: *The Journal of chemical physics* 103.11 (1995), pp. 4586–4599.

[9] Bogumil Jeziorski and Krzysztof Szalewicz. "Intermolecular interactions by perturbation theory". In: *Encyclopedia of computational chemistry* 2 (1998), p. 1376.

[10] Cercis Morera-Boado and Margarita I Bernal-Uruchurtu. "Interaction energy of Cl2 and Br2 with H2O: Exchange, dispersion and density the crucial ingredients". In: *Journal of Computational Chemistry* 44.10 (2023), pp. 1073–1087.

[11] Edward G Hohenstein and C David Sherrill. "Wavefunction methods for noncovalent interactions". In: *Wiley Interdisciplinary Reviews: Computational Molecular Science* 2.2 (2012), pp. 304–326.

[12] Konrad Patkowski. "Recent developments in symmetry-adapted perturbation theory". In: *Wiley Interdisciplinary Reviews: Computational Molecular Science* 10.3 (2020), e1452.

[13] Trent M Parker et al. "Levels of symmetry adapted perturbation theory (SAPT). I. Efficiency and performance for interaction energies". In: *The Journal of chemical physics* 140.9 (2014).

[14] John M Herbert. "Neat, simple, and wrong: Debunking electrostatic fallacies regarding noncovalent interactions". In: *The Journal of Physical Chemistry A* 125.33 (2021), pp. 7125–7137.

[15] Ka Un Lao and John M Herbert. "Energy decomposition analysis with a stable charge-transfer term for interpreting intermolecular interactions". In: *Journal of Chemical Theory and Computation* 12.6 (2016), pp. 2569–2582.

[16] John M Herbert and Kevin Carter-Fenk. "Electrostatics, charge transfer, and the nature of the halide–water hydrogen bond". In: *The Journal of Physical Chemistry A* 125.5 (2021), pp. 1243–1256.

[17] Fritz London. "The general theory of molecular forces". In: *Transactions of the Faraday Society* 33 (1937), 8b–26.

[18] Kevin Carter-Fenk, Ka Un Lao, and John M Herbert. "Predicting and understanding non-covalent interactions using novel forms of symmetry-adapted perturbation theory". In: *Accounts of Chemical Research* 54.19 (2021), pp. 3679–3690.

[19] *TURBOMOLE V7.2 2017, a development of University of Karlsruhe and Forschungszentrum Karlsruhe GmbH, 1989-2007, TURBOMOLE GmbH, since 2007; available from* `http://www.turbomole.com`.

[20] Daniel GA Smith et al. "PSI4 1.4: Open-source software for high-throughput quantum chemistry". In: *The Journal of chemical physics* 152.18 (2020).

[21] Shigekazu Kumakura, Fujiko Iwasaki, and Yoshihiko Saito. “The crystal structure of the 1: 1 complex of naphthalene with 1, 2, 4, 5-tetracyanobenzene”. In: *Bulletin of the Chemical Society of Japan* 40.8 (1967), pp. 1826–1833.